Decoupling of Multi-Element MIMO Antennas

Min Li and L. J. Jiang
Department of Electrical and Electronic Engineering
The University of Hong Kong
Hong Kong, China

***Abstract*—An efficient decoupling technique for multi-element MIMO antennas is proposed in this paper. A general model of using parasitic decoupling structure (PDS) to satisfy the criterions derived from antenna impedances for perfect isolation is presented. A prototype of three monopole antennas is realized on a Rogers PCB for demonstration purpose. The simulation results show that good impedance matching and high port isolation are achieved simultaneously.**

Keywords—Decoupling technique, multiple antennas, MIMO antenna, mutual coupling, isolation

I. Introduction

The next-generation (5G) wireless communication systems are on the way for high speed wireless data access [1]. Massive multiple-input multiple-output (MIMO) technique adopting multiple antenna elements is considered as one of the key enabling techniques for 5G networks. However, for a MIMO system with limited space for antennas' installing, the mutual couplings among the antenna elements cause interference and so have serious effect on the service performance. To confront this problem, various decoupling techniques (DTs) have been presented in the last few years [2-6]. While there are only a few literatures focusing on decoupling of multi-element MIMO (M-MIMO) antennas (antenna number $n\geq 3$), since it is much more challenging than implementing decoupling for two antennas. High isolation is attainable when antennas possess orthogonal and diversiform polarizations [2, 3]. However, this kind of DTs require arranging antennas at specific orientations and are not appealing for some applications. Electromagnetic band gap (EBG) structures [4] and split-ring resonators (SRRs) [5] have been widely applied for antennas' mutual coupling suppression. However, the drawbacks are the required large physical spacing, the complicated fabrication process and the caused negative effects. It is also a common DT of incorporating with some sorts of passive elements for mutual coupling suppression [6]. However, the inevitable optimization process could be labor intensive.

In this paper, we proposed an efficient DT for M-MIMO antennas. A general model of using parasitic decoupling structure (PDS) to satisfy the criterions derived from antenna impedances for perfect isolation is presented. The PDS is used to generate required interference against the original couplings among M-MIMO antennas for isolation enhancement.

II. Decoupling Theory

A. Parasitic Decoupling Structure

The decoupling setups for an M-MIMO antenna using the proposed PDS is sketched in Fig. 1. The "black box" consists of $(n^2+n)/2$ antenna scatterers, including n active antennas, denoted as Ants 1-n, and $(n^2-n)/2$ parasitic scatterers, denoted as P1-P$(n^2-n)/2$, individually implemented in between each antenna pair. The parasitic scatterers are passive elements and terminated by reactive loads with reactances of $\left\{Z_{L1}, Z_{L2}, \ldots Z_{L(n^2-n)/2}\right\}$. The transmission lines (TLs) are with same characteristic impedances of Z_0 (normally equal to 50 Ω) and electrical lengths of $\left\{\theta_1, \theta_2, \ldots \theta_{(n^2+n)/2}\right\}$, including the TLs of $\left\{\theta_1, \theta_2, \ldots \theta_n\right\}$ connected with the feed lines of the n active antennas and TLs of $\left\{\theta_{n+1}, \theta_{n+2}, \ldots \theta_{(n^2+n)/2}\right\}$ connected with the $(n^2-n)/2$ parasitic scatterers. The complete PDS is composed of the $(n^2-n)/2$ parasitic scatterers, the $(n^2+n)/2$ TLs, and the $(n^2-n)/2$ reactive loads.

B. Decoupling Procedures

The decoupling procedures can be formulated into the following four steps.

Step 1: Insert the parasitic scatterers individually in between each antenna pair and obtain the scattering matrix $[S^{t1}]$ of the $(n^2+n)/2$–port network at the reference plane t_1. For n active antennas, the total required number of parasitic scatterers is $C_n^2 = (n^2-n)/2$, while in practice, the number can be reduced a lot due to symmetrical configuration.

Step 2: Insert the TLs to feed lines of the antennas and parasitic scatterers to introduce phase delays $\boldsymbol{\theta} = \left\{\theta_1, \theta_2, \ldots \theta_{(n^2+n)/2}\right\}$ for the $(n^2+n)/2$–port network and obtain the new scattering matrix $[S^{t2}]$ at t_2.

Step 3: Terminate the parasitic scatterers by reactive loads with reactances of $\mathbf{Z_L} = \left\{Z_{L1}, Z_{L2}, \ldots Z_{L(n^2-n)/2}\right\}$ to obtain the scattering matrix $[S^{t3}]$ at t_3.

Step 4: Use the computed $\boldsymbol{\theta}$ and $\mathbf{Z_L}$ in Step 3 to obtain the input impedances of the decoupled antennas to implement matching networks and obtain the scattering matrix $[S^{t4}]$ at t_4.

The decoupling purpose is to eliminate the mutual coupling, hence the following decoupling conditions should be satisfied.

$$Z_{Ai,Aj}^{t_3} = 0,\ \left\{Z_{Ai,Aj}^{t_3} \in \mathbf{Z}^{\mathbf{t_3}}, i \neq j \in [1,\ n]\right\}. \tag{1}$$

According to the parasitic decoupling theory, the variables $\boldsymbol{\theta} = \left\{\theta_1, \theta_2, \ldots \theta_{(n^2+n)/2}\right\}$ and $\mathbf{Z_L} = \left\{Z_{L1}, Z_{L2}, \ldots Z_{L(n^2-n)/2}\right\}$ introduced by the PDS can be precisely determined to eliminate the mutual coupling, i.e., equation (1).

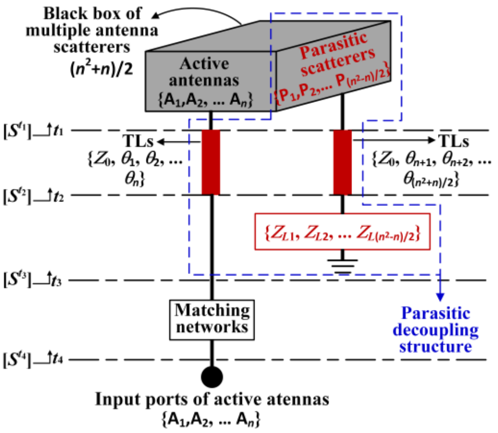

Fig. 1 Decoupling setups for M-MIMO antennas.

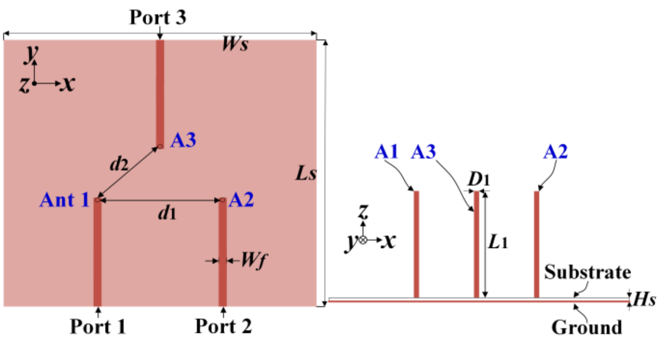

(a) (b)

Fig. 2 (a) top view and (b) side view of the three coupled monopoles (metal in front and metal in bottom).

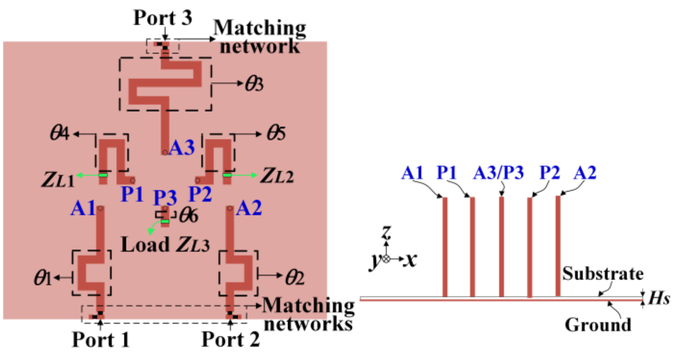

(a) (b)

Fig. 3 (a) top view and (b) side view of the three decoupled monopoles using the PDS (metal in front and metal in bottom).

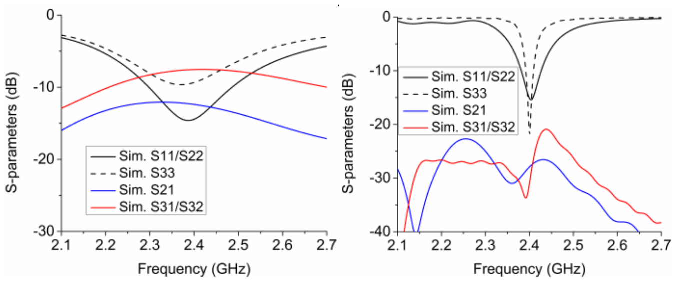

(a) (b)

Fig. 4 Simulated S-parameters of: (a) the coupled and (b) the decoupled monopole arrays.

III. Decoupling Example

A. Antenna Configuration

Fig. 2 shows three coupled monopoles (Ants 1, 2 and 3), with same lengths of L_1 =29 mm, diameters of D_1=1.0 mm and separations of d_1=28 mm=0.22λ_0 and d_2=18.5 mm=0.15λ_0. The antennas are designed on a 60 mm×70 mm (Ls×Ws) Rogers RO 4350 substrate. The configuration of the final design with using the present PDS is shown in Fig. 3. Three simple *L*-section impedance matching circuits consisting of a series inductor (2.9 nH) with a shunt capacitor (2.0 pF), a series inductor (2.9 nH) with a shunt capacitor (2.0 pF) and a series capacitor (1.6 pF) with a shunt capacitor (2.1 pF), are adopted individually at each antenna input port for matching purpose. The other relevant parameters are $\boldsymbol{\theta}=\{\theta_1,\theta_2,\theta_3,\theta_4,\theta_5,\theta_6\}=\{0.61, 0.61, 2.15, 1.23, 1.23, 0.23\}$and $\mathbf{Z_L}=\{Z_{L1},Z_{L2},Z_{L3}\}=\{-j82.8,-j82.8, j13.6\}$.

B. Simulation Results

The isolations of the coupled and decoupled monopoles, as well as the return loss for each antenna port are both shown in Fig. 4. It can be seen from Fig. 4(a) that the port isolations among the three coupled antennas, as indicated by S_{21} and S_{31}, are only ~7 dB and ~12 dB, respectively, at the frequency of 2.4 GHz. It can be observed from Figs. 4(a) and 4(b) that by using the presented PDS, the port isolations are significantly improved to around 28 dB at 2.4 GHz. Moreover, Fig. 4(b) also shows good impedance matching, indicated by S_{11}, S_{22} and S_{33}, for each antenna input port.

IV. Conclusion

This paper presented an efficient decoupling technique for M-MIMO antennas. The general model of PDS was presented. A prototype of three monopole antennas was realized on a Rogers PCB for demonstration purpose. The simulated results demonstrated that isolations of more than 25 dB were achieved by using the presented PDS.

References

[1] Z. S. Zhang, X. Y. Wang, K. P. Long, A. V. Vasilakos and L. Hanzo, "Large-scale MIMO-based wireless backhaul in 5G networks," IEEE Wireless Commun., vol. 22, no. 5, pp. 58-66, Oct. 2015.

[2] M. Li, Q. L. Li, B. Wang, C. F. Zhou and S. W. Cheung, "A low-profile dual-polarized dipole antenna using wideband AMC reflector," IEEE Trans. Antennas Propag., vol. PP, no. 99, pp. 1-1, 2018. (Early access)

[3] A. S. Konanur, K. Gosalia, S. H. Krishnamurthy, B. Hughes, and G. Lazzi, "Increasing wireless channel capacity through MIMO systems employing co-located antennas," IEEE Trans. Microw. Theory Tech., vol. 53, pp. 1837–1844, Jun. 2005.

[4] F. Yang and Y. R. Samii, "Microstrip antennas integrated with electromagnetic band-gap EBG structures: A low mutual coupling design for array applications," IEEE Trans. Antennas Propag., vol. 51, no. 10, pp. 2936-2946, Oct. 2003.

[5] A. Habashi, J. Nourinia and C. Ghobadi, "Mutual coupling reduction between very closely spaced patch antennas using low-profile folded split-ring resonators (FSRRs)," IEEE Antennas Wireless Propag. *Lett.*, vol. 10, no. , pp. 862-865, 2011.

[6] A. C. K. Mak, C. R. Rowell, and R. D. Murch, "Isolation enhancement between two closely packed antennas," IEEE Trans. Antennas Propag., vol. 56, no. 11, pp. 3411–3419, Nov. 2008.